Optical Larmor Beat Detection of High-Resolution Nuclear Magnetic Resonance in a Semiconductor Heterostructure

J. A. Marohn, P. J. Carson, J. Y. Hwang, M. A. Miller, D. N. Shykind, and D. P. Weitekamp
Arthur Amos Noyes Laboratory of Chemical Physics, M/S 127-72, California Institute of Technology, Pasadena, California 91125
(Received 20 March 1995)

A new method of optical nuclear magnetic resonance, Larmor beat detection, is described and demonstrated on a III-V semiconductor heterostructure. Modulation of the circular polarization of luminescence at the difference between two nuclear spin precession frequencies is induced by rf pulses. One isotope provides a spin-locked reference field, while NMR transients of a second isotope are observed optically in real time. Order-of-magnitude improvement in resolution and sensitivity over previous techniques is obtained, revealing weak electric field gradients in single epitaxial structures.

PACS numbers: 73.20.Dx, 76.60.–k, 78.55.–m, 78.66.Fd

In principle, solid-state nuclear magnetic resonance (NMR) should be a valuable tool in structural studies of semiconductor quantum wells and heterostructures. For example, it has been proposed that the isotropic optically induced Knight shift of the NMR resonance frequency [1–3] could be used to map the excited state electronic wave function of a quantum well with atomic resolution [4]. Splittings due to the quadruple interaction of nuclei with electric field gradients, measured by NMR, have been attributed to strain in GaAs quantum wells [5] and to localized defects in bulk GaAs [6]. In analogy to observations on bulk GaAs [7], gradients at the nucleus should also be induced by electric fields, allowing their localized measurements.

In practice, conventional NMR has proven incapable of probing single epitaxial structures both because of the small equilibrium magnetizations ordinarily achieved and because of the low sensitivity inherent in detection by magnetic induction of precessing magnetization [8]. Large nonequilibrium nuclear magnetization may be obtained in a semiconductor by optically pumping interband transitions with circularly polarized light [9,10] and has allowed pulsed NMR in stacked arrays of quantum wells by conventional magnetic induction [11]. Quasi-steady-state optical detection of nuclear magnetization through an excited state Hanle effect [10] provides another sensitivity boost [10,12] and has made possible low resolution cw NMR of individual epitaxial structures [3,5]. Separating the processes of optical pumping, NMR, and optical detection into distinct periods of time in the optical NMR experiment [2,4,6] proved necessary to obtain spectral resolution equal to that of conventional time-domain NMR. However, unlike conventional NMR, such time-sequenced optical NMR requires field cycling and point-wise acquisition of the desired interferogram.

We report here a new optical NMR experiment, Larmor beat detection (LBD), which lifts these restrictions and allows for the *real-time* optical detection of NMR transients in semiconductors at fixed magnetic field. The LBD method relies on the depolarization of semiconductor luminescence by two precessing nuclear hyperfine fields: a reference field $\mathbf{B}_N^{\mathrm{ref}}$ and a signal field $\mathbf{B}_N^{\mathrm{sig}}$, corresponding to distinct nuclear species. Irradiation with circularly polarized light creates carriers with a large nonequilibrium electron spin-polarization vector $\mathbf{P}_e$ along the static Zeeman field $\mathbf{B}_0$ [1]. The degree of circular polarization ρ of subsequent luminescence measures the average component of this electron spin polarization in the direction of observation [10]. Electron spin-lattice relaxation competes with the optical decay of the excited state to establish within nanoseconds a steady-state value ρ_0 of luminescence polarization. In the presence of transverse magnetic fields, $\mathbf{P}_e$ is reoriented and diminished, reducing the observed ρ. Here the transverse magnetic field is dominated by the total transverse nuclear hyperfine field, $\mathbf{B}_N^{\mathrm{tot}} = \mathbf{B}_N^{\mathrm{sig}} + \mathbf{B}_N^{\mathrm{ref}}$, where $\mathbf{B}_N^{\mathrm{sig}}$ will be due to ^{71}Ga or ^{69}Ga and $\mathbf{B}_N^{\mathrm{ref}}$ to ^{75}As.

The modulation of luminescence polarization may be quantified by solving the steady-state Bloch equation governing $\mathbf{P}_e$ [13] for the new case of two single-frequency, circularly polarized nuclear hyperfine fields. With the difference in Larmor frequencies given by $\omega = \omega_{\mathrm{sig}} - \omega_{\mathrm{ref}}$, we calculate

$$\rho = \rho_0 \frac{1}{1 + (b_N^{\mathrm{ref}})^2 + (b_N^{\mathrm{sig}})^2 + 2 b_N^{\mathrm{ref}} b_N^{\mathrm{sig}} \cos\omega t}, \quad (1)$$

where the transverse nuclear field magnitudes in reduced units are defined as

$$b_N^k = \left(\frac{(B_{N,x}^k)^2 + (B_{N,y}^k)^2}{B_H^2 + (\mathbf{B}_0 + \mathbf{B}_N^{\mathrm{misc}})^2} \right)^{1/2} \quad (k = \mathrm{ref},\ \mathrm{sig}). \quad (2)$$

The denominator in Eq. (2) includes the net miscellaneous nuclear hyperfine field components $\mathbf{B}_N^{\mathrm{misc}}$ remaining along the z axis, which add vectorially to $\mathbf{B}_0$. The Hanle width, $B_H = 1/\gamma_e \tau$ is the inverse lifetime $(1/\tau)$ of the oriented electron converted to field units through its gyromagnetic ratio γ_e. The denominator in Eq. (1) neglects applied rf fields, which are much smaller than $\mathbf{B}_N^{\mathrm{sig}}$ or $\mathbf{B}_N^{\mathrm{ref}}$. Equation (1) with $\mathbf{B}_N^{\mathrm{ref}} = 0$ reduces to the well-known

 0031-9007/95/75(7)/1364(4)$06.00

[10] Lorentzian describing the Hanle-effect depolarization of ρ by a single transverse field $\mathbf{B}_N^{\text{sig}}$.

In order to generalize this result to an arbitrary signal spectrum, it is convenient to isolate the components of this response that are linear in an arbitrary set of signal fields $b_N^{\text{sig},i}$, where i indexes lines in the spectrum, including lines from more than one signal isotope when applicable. Expanding a generalized version of Eq. (1) in a sum of Taylor series about $b_N^{\text{sig},i} = 0$ and assuming $b_N^{\text{sig},i} \ll b_N^{\text{ref}}$ gives

$$\rho(t) = -2\rho_0 \sum_i \left(\frac{b_N^{\text{ref}}(t)}{\{[b_N^{\text{ref}}(t)]^2 + 1\}^2} b_N^{\text{sig},j}(t) + O((b_N^{\text{sig},i})^3) \right) \cos\omega_i t , \quad (3)$$

where $\omega_i = \omega_{\text{sig},i} - \omega_{\text{ref}}$ and where only term linear in $\cos\omega_i t$ are kept. Linear response with good sensitivity requires that $b_N^{\text{ref}} \approx 1$ and $b_N^{\text{sig},i} \ll 1$. Note that the aggregate spectral width of the beat frequencies need only be $\ll 1/\tau$ for the steady-state electron Bloch equation to apply, providing a bandwidth of many MHz. As written in Eq. (3), the time dependence of the magnitudes b_N^{ref} and $b_N^{\text{sig},i}$ is due to the transverse relaxation for each separate nuclear hyperfine field. With weak irradiation or with spin locking, b_N^{ref} changes slowly ($T_{1\rho} \sim 1$ s) compared to the decay of $b_N^{\text{sig},i}$ (<1 ms). Under these conditions, the Fourier components of ρ near the beat frequencies are essentially those present in the transients of the *signal* nuclei alone.

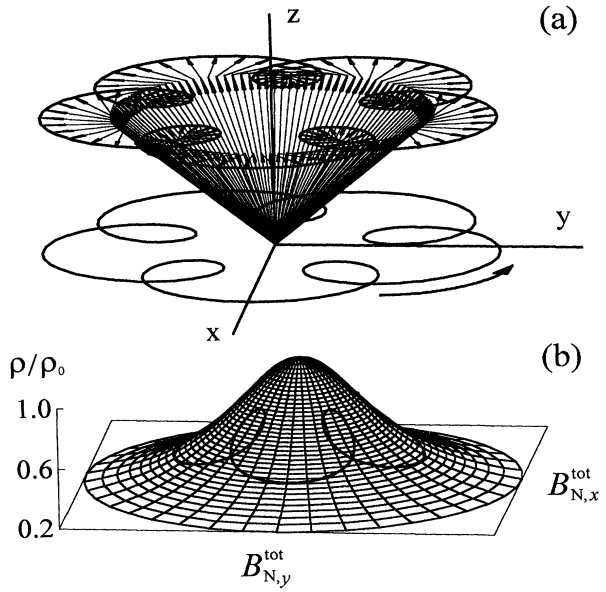

FIG. 1. (a) Schematic depiction of the evolution of ^{71}Ga and ^{75}As nuclear hyperfine fields during Larmor beat detection. The "reference" field (^{75}As) is shown precessing in a cone about the z axis defined by the static magnetic field (not shown), in steady-state response to weak off-resonance irradiation, the "signal" field (^{71}Ga) is shown as a purely transverse field precessing about the static field. The vector sum of the two fields is shown as an elevated rosette, and its projection, of relevance to the Hanle effect, is shown in the x-y plane. (b) The transverse component of the vector sum trajectory is shown projected onto the 2D Hanle curve describing luminescence depolarization. The vertical component of the projected curve gives ρ, which now oscillates, primarily at the Larmor beat frequency.

Figure 1 illustrates schematically the orientations for the signal and reference nuclear hyperfine fields during Larmor beat detection. The spin-locked ^{75}As reference field plays a dual role: Its transverse component provides b_N^{ref}, while its longitudinal component helps increase detection sensitivity for $\mathbf{B}_N^{\text{sig}}$ by contributing to $\mathbf{B}_N^{\text{misc}}$ in a direction antiparallel to the applied Zeeman field, thereby reducing the denominator in Eq. (2).

Figure 2 shows a real-time ^{71}Ga free induction decay (FID) recorded using optical Larmor beat detection and the timing sequence SAT-τ_L-$\pi/2$-DET. Here SAT represents a train of ten $\pi/2$ pulses (10 ms apart) applied to each of the principal isotopes (^{69}Ga, ^{71}Ga, and ^{75}As) to provide a reproducible condition of saturation or null spin order before each shot. A period τ_L of optical nuclear polarization is followed by a $\pi/2$ pulse delivered to ^{71}Ga, and DET represents Larmor beat detection of the ^{71}Ga NMR free induction decay during weak ^{75}As irradiation off resonance.

As in ordinary NMR, the 1D real-time FID experiment has sensitivity inferior to an analogous 2D experiment in which spin locking is used to prolong the transverse signal magnetization [14]. Here the sequence needed is SAT-τ_L-$(\theta)_\phi$-t_1-DET, in which an on-resonance pulse of tip angle θ and phase ϕ induces free evolution during t_1 and detection is prolonged by spin locking of the remaining ^{71}Ga magnetization while irradiating the reference ^{75}As isotope

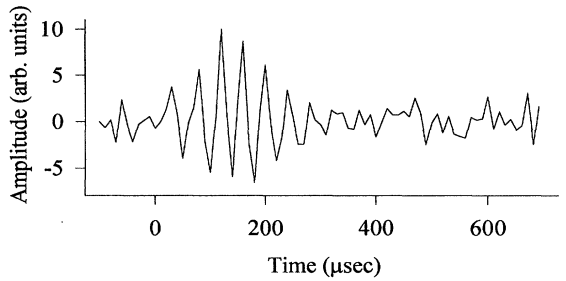

FIG. 2. Real-time optical detection of the ^{71}Ga free induction decay in a GaAs heterojunction. Following $\tau_L = 5$ s of optical nuclear polarization, a 3.6 μs, 3.152 MHz, $\pi/2$ pulse to ^{71}Ga at time zero creates the transverse nuclear "signal" field. A 0.6 mT, 1.824 MHz ^{75}As spin lock 54 kHz off resonance provides the transverse "reference" field. Luminescence polarization, sampled during free evolution and demodulated by a frequency near the Larmor beat frequency, is digitized to give the observed transient. The transient shown represents 100 averages taken in 10 min total time. The transient's rise time is due to filter response.

during t_2 (DET). The optical transient in DET, now at the difference in irradiation frequencies, is demodulated, integrated, and plotted versus t_1 to yield the desired NMR interferogram. By inserting a π pulse at $t_1/2$ we may record the spin-echo interferogram, and by extending the pulse the full length of t_1 we may record a nutation transient. The signal-to-noise ratio per shot improves in these 2D experiments by $\sim(T_{1\rho}/T_2)^{1/2}$ since the signal persists for the spin-locking time $T_{1\rho}$ ($\sim$1 s) instead of the decay time T_2 for the FID ($\sim$100 μs). The spectrum of interest can be shifted away from artifacts due to drifts in the total signal amplitude by applying time proportional phase incremenation (TPPI) [15], in which the phase of the on-resonance preparation pulse is stepped according to $\phi = \omega_{\mathrm{TPPI}} t_1$.

The sample studied was a single p-channel GaAs/AlGaAs heterojunction grown along the [001] axis by molecular beam epitaxy [3,16]. A substrate of semi-insulating GaAs supports a 2500 nm layer of undoped GaAs, followed by a 6.5 nm layer of undoped $Al_xGa_{1-x}As$ ($x = 0.36$), a 30 nm layer of p-type $Al_xGa_{1-x}As$ ($x = 0.36$) doped with $6 \times 10^{17}/cm^3$ of Be, and a 21 nm layer of undoped GaAs. The photoluminescence spectrum of the sample reveals the expected lines at 818 nm (bulk exciton luminescence) [3], and 825 and 830 nm (e line and d line, respectively, of H-band luminescence) [16], which have been assigned to transitions involving the recombination with electrons of the 2D heavy holes localized near the interface between GaAs and undoped AlGaAs.

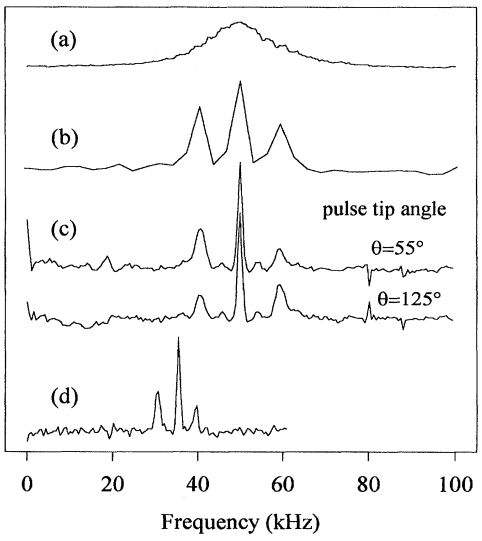

FIG. 3. Optical NMR spectra of the heterostructure. (a) Steady-state cw ^{71}Ga optical NMR spectrum (see text). (b) Fourier transform of ^{71}Ga free induction decay in t_1 following a $\theta = \pi/2$ pulse, recorded by Larmor beat detection in t_2. (c) Spin-echo spectrum. (d) Nutation spectrum. Each spectrum (b)–(d) results from a t_2 transient at each t_1 point, with the entire set of transients taken in 30 min.

The sample was attached by high vacuum grease (Fig. 2) or varnish (Fig. 3) to a G-10 fiberglass probe immersed in 2 K superfluid ^{4}He. The 240 mT Zeeman field, optical detection axis, and sample growth axis were nominally parallel. A GaAs/AlGaAs laser diode delivered $\sim$5 mW cw of circularly polarized 780 nm light over $\sim$1 mm^2, incident 15° off axis. Sample luminescence passed through a 50 kHz photoelastic modulator, a linear polarizer, and 830 nm bandpass filter (FWHM 10 nm), and was detected with a silicon avalanche photodiode in linear mode. For steady-state experiments, the photocurrent was demodulated by 50 kHz. For Larmor beat experiments, the photocurrent was demodulated by 50 kHz plus the relevant beat frequency. The demodulated signal, proportional to the time-dependent difference in intensity between left and right circularly polarized luminescence, was digitized.

As a point of reference, Fig. 3(a) shows the quasi-steady-state cw ^{71}Ga optical NMR spectrum ($\tau_L = 30$ s) of the heterostructure, reproducing the result of Ref. [3] on our sample. The signal grows in during optical nuclear polarization with a time constant of 500 s. This steady-state spectrum is featureless even for ^{71}Ga Rabi frequencies small compared to the dipolar local field, while in contrast the Fourier transform ($\tau_L = 5$ s) of the ^{71}Ga FID recorded using Larmor beat detection shows a well-resolved triplet [Fig. 3(b)]. Since a spin-echo experiment [Fig. 3(c)] refocuses evolution due to static field inhomogeneity, chemical shifts, and heteronuclear dipolar couplings, the surviving triplet structure is shown to be due to quadrupole coupling. Splittings observed in the ^{69}Ga spectra (not shown) scale with nuclear quadrupole moment, verifying this conclusion. The nutation spectrum [Fig. 3(d)] in which the triplet splitting is half as large also verifies a quadrupole coupling and reveals an ω_1 of 35.1 kHz (where $\omega_1 = \gamma_N^{\mathrm{sig}} B_1$ and B_1 is the magnitude of the circular component of the applied rf field). The lack of a peak at 52.6 kHz, where $2\omega_1$ would fold into the nutation spectrum, proves that there are no strongly quadrupole-perturbed sites ($\omega_Q \gg \omega_1$) contributing to the spectrum.

The spectra of Figs. 3(b)–3(d) are consistent with a roughly Gaussian distribution of ^{71}Ga quadrupole splittings (mean splitting of -18.6 ± 0.1 kHz and FWHM of 4.6 ± 0.3 kHz), corresponding to an electric field gradient whose principal component along [001] is $V_{zz} = -6.76 \times 10^{18}$ V/m^2 (where the sign is obtained as discussed below). The mean quadrupole splitting varied from 12 to 20 kHz between Dewar cooling cycles.

An electric field gradient (EFG) can be induced at a nuclear site in GaAs when its tetrahedral symmetry is broken due to local bonding effects (inconsistent with the observed narrow distribution of quadrupole couplings) as

well as by changes in electron distribution due to strain [17] induced by lattice mismatch or external pressure. Quadrupole couplings observed previously in quantum wells have been attributed to external strain such as that developed in a rigidly mounted sample upon cooling [5]. Assuming that our splittings are due to external strain perpendicular to [001], we infer a strain of 70 ppm and in turn a pressure of 8.2×10^6 Pa (0.082 kbar). An EFG can also be induced by electric fields [7]. Symmetry arguments show, however, that an electric field $E_{[001]}$ (such as the built-in electric field of the heterojunction) in a cubic crystal gives rise to an EFG whose principal component along [001] vanishes, so that varying the angle between $\mathbf{B}_0$ and [001] would be required to measure $E_{[001]}$. Since a ^{69}Ga quadrupole splitting as small as 1.0 kHz is resolvable, the current technique, modified to allow variation of the angle between $\mathbf{B}_0$ and crystal axes, could be used to sort out these contributions and thus to measure internal electric fields with a resolution of 50 kV/m and strains as small as 4 ppm in a single heterojunction.

The dependence of the satellite ratios on preparation-pulse tip angle θ measures the ^{71}Ga nuclear spin polarization (and reveals the sign of V_{zz} [18]). Assuming a single spin temperature, the satellite ratios measured as a function of θ indicate nuclear spin polarizations on the order of -10%. The calculated polarization enhancement due to ONP is approximately 2000.

Larmor beat detection bears a superfluid resemblance to optically pumped NMR detected via a gas-phase alkali-halide magnetometer [19]. That experiment relies on a time-dependent *linearly* polarized transverse reference field and uses a *ground-state* Hanle effect to observe small real-time changes in transverse ("signal") fields. The large nuclear hyperfine reference field and relatively short electron spin lifetime allow the present method to work at far higher static fields, with bandwidth large enough for real-time solid-state NMR.

In conclusion, optical Larmor beat detection makes use of two precessing nuclear hyperfine fields to convert the excited-state Hanle effect into a high-sensitivity linear optical NMR, method capable of real-time detection. The method applies to all samples where optical NMR by the Hanle effect is observable for two nuclear hyperfine fields, each comparable to the larger of the static field or Hanle width, a prerequisite satisfied by many known samples up to static fields of greater than 1 T [2–6,10]. In addition to an orders-of-magnitude sensitivity advantage over magnetic induction, it allows improved sensitivity and an orders-of-magnitude resolution advantage relative to steady-state optical NMR techniques. Arbitrary pulsed NMR techniques can be adapted and the resulting transients observed in real time or with spin-locked detection.

This work was funded by the NSF program in Materials Synthesis and Processing and by NASA through the Caltech President's Fund. We thank A. Ksendzov, J. Liu, and F. Grunthaner of the NASA Jet Propulsion Laboratory's Center for Space Microelectronics Technology for sample preparation and luminescence characterization, and L. Burnett and A. Perry for cryogenics advice.

[1] D. Paget, G. Lampel, B. Sapoval, and V. I. Safarov, Phys. Rev. B **15**, 5780 (1977).
[2] S. K. Buratto, D. N. Shykind, and D. P. Weitekamp, Phys. Rev. B **44**, 9035 (1991).
[3] M. Krapf, G. Denninger, H. Pascher, G. Weimann, and W. Schlapp, Solid State Commun. **78**, 459 (1991).
[4] S. K. Buratto, D. N. Shykind, and D. P. Weitekamp, J. Vac. Sci. Technol. B **10**, 1740 (1992).
[5] G. P. Flinn, R. T. Harley, M. J. Snelling, A. C. Tropper, and T. M. Kerr, Semicond. Sci. Technol. **5**, 533 (1990).
[6] S. K. Buratto, J. Y. Hwang, N. D. Kurur, D. N. Shykind, and D. P. Weitekamp, Bull. Magn. Res. **15**, 190 (1993).
[7] N. Bloembergen, Proc. Colloq. Ampere (Atomes Mol. Etudes Radio Elec.) **11**, 39–57 (1962).
[8] A. Abragam, *Principles of Nuclear Magnetism* (Clarendon Press, Oxford, 1961).
[9] G. Lampel, Phys. Rev. Lett. **20**, 491 (1968).
[10] *Optical Orientation,* edited by F. Meier and B. P. Zakharchenya (Elsevier, Amsterdam, 1984).
[11] S. E. Barrett, R. Tycko, L. N. Pfeiffer, and K. N. West, Phys. Rev. Lett. **72**, 1368–1371 (1994).
[12] A. I. Ekimov and V. I. Safarov, Pis'ma Zh. Eksp. Teor. Fiz. **15**, 543 (1972) [JETP Lett. **15**, 319 (1972)].
[13] V. G. Fleisher and I. A. Merkulov, in *Optical Orientation,* edited by F. Meier and B. P. Zakharchenya (Elsevier, Amsterdam, 1984).
[14] D. P. Weitekamp, Adv. Magn. Res. **11**, 197 (1983).
[15] G. Drobny, A. Pines, S. Sinton, D. P. Weitekamp, and D. Wemmer, Symp. Faraday Soc. **13**, 49 (1979).
[16] W. Ossau, E. Bangert, and G. Weimann, Solid State Commun. **64**, 711 (1987); Y. R. Yuan, M. A. A. Pudensi, G. A. Vawater, and J. L. Merz, J. Appl. Phys. **58**, 397 (1985).
[17] R. K. Sundfors, Phys. Rev. B **10**, 4244–4252 (1974).
[18] P. L. Kuhns and J. S. Waugh, J. Chem. Phys. **97**, 2166–2169 (1992).
[19] C. Cohen-Tannoudji, J. Dupont-Roc, S. Haroche, and F. Laloe, Rev. Phys. Appl. **5**, 95–101 (1970); Z. Wu, W. Happer, and J. M. Daniels, Phys. Rev. Lett. **59**, 1480 (1987).